Liquid Crystals
Publication details, including instructions for authors and subscription information:
http://www.informaworld.com/smpp/title~content=t713926090

FTIR spectroscopy of smectic elastomer films under lateral strain

Victor Aksenov[a]; Ralf Stannarius[a]; Michael Tammer[b]; Patrick Kölsch[b]; Friedrich Kremer[b]; Martin Rössle[c]; Rudolf Zentel[c]
[a] Otto-von-Guericke-Universität Magdeburg, Institut für Experimentelle Physik, D-39106 Magdeburg, Germany [b] Universität Leipzig, Institut für Experimentelle Physik I, D-04103 Leipzig, Germany [c] Universität Mainz, Institut für Organische Chemie, D-55099 Mainz, Germany

To cite this Article Aksenov, Victor , Stannarius, Ralf , Tammer, Michael , Kölsch, Patrick , Kremer, Friedrich , Rössle, Martin and Zentel, Rudolf(2007) 'FTIR spectroscopy of smectic elastomer films under lateral strain', Liquid Crystals, 34: 1, 87 — 94
To link to this Article: DOI: 10.1080/02678290601020104
URL: http://dx.doi.org/10.1080/02678290601020104

Liquid Crystals, Vol. 34, No. 1, January 2007, 87–94

Taylor & Francis
Taylor & Francis Group

FTIR spectroscopy of smectic elastomer films under lateral strain

VICTOR AKSENOV*†, RALF STANNARIUS†, MICHAEL TAMMER‡, PATRICK KÖLSCH‡, FRIEDRICH KREMER‡, MARTIN RÖSSLE§ and RUDOLF ZENTEL§

†Otto-von-Guericke-Universität Magdeburg, Institut für Experimentelle Physik, Universitätsplatz 2, D-39106 Magdeburg, Germany

‡Universität Leipzig, Institut für Experimentelle Physik I, Linnéstrasse 5, D-04103 Leipzig, Germany

§Universität Mainz, Institut für Organische Chemie, Duesbergweg 10–14, D-55099 Mainz, Germany

(*Received 21 March 2006; in final form 31 July 2006; accepted 10 August 2006*)

Polarized Fourier transform infrared (FTIR) spectroscopy is used to study the strain-induced compression of molecular layers in oriented smectic liquid crystal elastomer films. A reversible change of the smectic layer thickness in SmA and SmC* films in response to external strain was revealed earlier by optical reflectometry and X-ray measurements. However, these methods cannot probe the mechanism of layer compression on a molecular level. Polarized FTIR spectra show that the induced mesogenic tilt, one of the possible mechanisms, is too small to provide the dominating contribution to the layer shrinkage. The FTIR absorbance spectra of stretched samples are also evidence that there are no significant changes of the order parameter. Apparently, layer compression is achieved by a certain interpenetration of neighbouring layers, and/or compression of the interstitial backbone and spacer layers.

1. Introduction

Liquid crystal elastomers (LCEs) have become an important object of experimental and theoretical investigations due to their unusual physical properties [1–18]. This class of material combines the rubber elasticity of polymers with the anisotropic properties of liquid crystals. The polymeric network couples microscopic characteristics, such as director orientation and order parameter, to the macroscopic shape and dimensions of LCEs. Due to this coupling, the modification of the mesogenic orientational distribution or order parameter can change the macroscopic dimensions of the elastomer [1–4] and, *vice versa*, changes of the macroscopic sample dimensions can influence the mesogen orientational distribution or order parameter. One of the most spectacular effects is the drastic shape change which can attain 100% and more at the order–disorder transitions. Owing to such unique properties, LCEs are candidates for diverse technical applications, for example as artificial muscles [5].

The main goal of this article is the experimental study of the influence of mechanical deformations on the mesogen orientation in a LCE by polarized FTIR spectroscopy. In general, ordered smectic LCEs possess anisotropic macroscopic mechanical properties. In some materials, uniaxial deformations in the plane of the smectic layers are similar to deformations of two-dimensional isotropic rubbers, and they are determined by the entropy elasticity of the polymer network. Elastic moduli in this case are expected to be of the same order of magnitude as in isotropic rubbers (or in the isotropic phase of the material). For deformations perpendicular to the smectic layers, elastic moduli of the order of magnitude of the smectic layer compression constant have been found experimentally [6]. They can thus be orders of magnitude larger than those for deformations in the smectic layer plane [6, 7]. For such materials, it is plausible to expect that a uniaxial stretching in the smectic layer plane does not cause deformations perpendicular to the smectic layers, but the sample will shrink in the smectic layer plane perpendicular to the stretching direction in order to preserve its volume [7]. The consequence is a Poisson ratio ν (ratio of the transversal contraction and longitudinal extension) close to unity in the smectic layer plane, and $\nu=0$ perpendicular to it.

By contrast, for the material studied in this work, it has been found that stretching of free-standing films in the SmA phase in the film plane induces a shrinkage of the film thickness, the measured Poisson ratio is isotropic and close to ½ [8]. The molecular interpretation of this behaviour is unresolved.

*Corresponding author.
Email: victor.aksenov@physik.uni-magdeburg.de

Liquid Crystals
ISSN 0267-8292 print/ISSN 1366-5855 online © 2007 Taylor & Francis
http://www.tandf.co.uk/journals
DOI: 10.1080/02678290601020104

Previous studies of the latter type of materials have been performed, e.g. using optical reflectometry, X-ray reflection and scattering, and NMR spectroscopy. While these methods provide detailed information on different aspects of the mechanical characteristics, an overall unambiguous understanding of the phase transitions, orientational order and deformations in the stretched LCE material on a molecular level has not yet been achieved. Optical reflectometry measurements yield only an integral optical thickness change [8, 10]. X-ray measurements allow one to define very precisely the individual layer thickness changes in SmA and SmC phases under deformation [8] and changes of the smectic layer thickness at phase transitions [12]. Simultaneous optical reflectometry and small angle X-ray scattering measurements have shown that, during stretching of thin films with layers parallel to the surface, the changes of optical thickness are consistent with the measured changes of the molecular layer spacing [8]. Real film thickness changes are in good agreement with the smectic layer compression derived from X-ray measurements, and with a Poisson ratio close to ½. It has been shown that mechanical deformation can cause a considerable compression (up to 30%) of smectic layers [8].

Neither optical reflectometry nor small angle X-ray scattering give information about molecular mechanisms. There are at least three possible scenarios of the smectic layers compression: the first is an induction of tilt of the mesogens, the second mechanism is layer interpenetration, and the third is a reduction of the orientational order of the mesogens. A method that can provide detailed information about mesogen orientation is NMR, but unfortunately this method is not appropriate for thin films, because it requires substantial amounts of material. Phase transitions in bulk samples of similar polymers (without crosslinker groups) were studied ^{13}C and ^{1}H NMR [13], and ^{13}C NMR was employed to study the temperature dependence of orientational order. Because the resonance frequency of an individual carbon site depends on the product of phase geometry $\frac{1}{2} <3\cos^2\varepsilon - 1>$ (where ε is the angle between the director and mesogen long axis, and brackets denote ensemble averaging), an alignment factor $\frac{1}{2}(3\cos^2\Phi - 1)$ with the angle Φ between director and external magnetic field, and the order parameter S, it is quite impossible to distinguish unambiguously these influences on the NMR spectra without model assumptions [13].

One suitable method for the study of thin liquid crystal elastomer films on a molecular level is polarized Fourier transform infrared (FTIR) spectroscopy. It allows the study of the molecular structure of soft materials in response to external forces such as electromagnetic field [14, 15, 19, 20] and mechanical strain [16, 21]. The main goal of this article is to explain the molecular mechanisms of the strain-induced compression of smectic layers in oriented smectic LCE samples by polarized FTIR spectroscopy.

2. Sample preparation and experiment

Elastomer films were prepared by crosslinking free-standing films of a precursor polymer. The chemical structure of the precursor is shown in figure 1. The precursor is a random side chain copolymer; it consists of a siloxane backbone with mesogen-substituted, crosslinker-substituted and non-substituted segments in ratios 0.95:0.05:2.7. The crosslinker groups have the same structure as the mesogenic substituents, except for a terminal photoreactive group.

The non-crosslinked polymer has the phase sequence SmX 65°C SmC* 95–96°C SmA 125°C. The elastomer films are produced by irradiation of free-standing polymer films using a 250 W Panacol-Elosol UV point source UV-P 280 in the SmA phase, following a

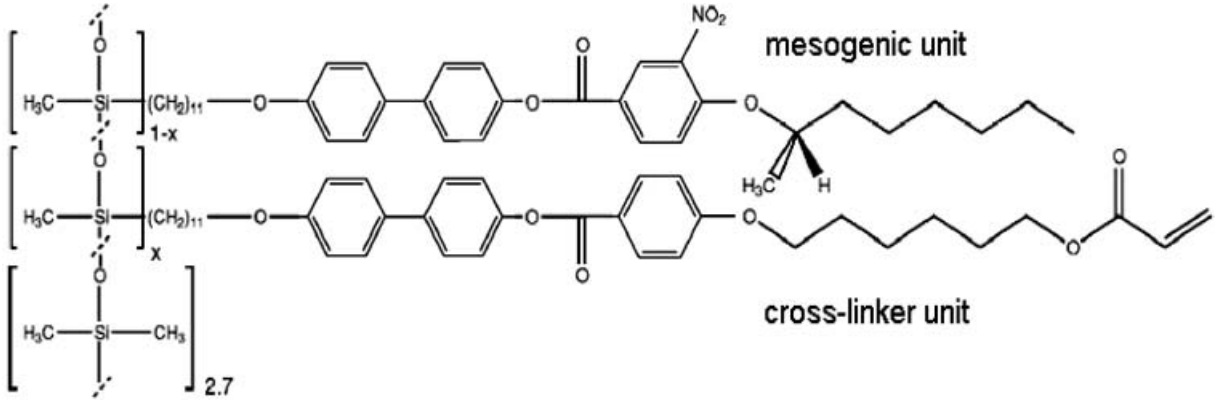

Figure 1. Chemical composition of the precursor copolymer, a three-kernel material with crosslinker fraction $x=0.05$.

procedure described in [8, 10]. In a first step, the two side edges of the film are covered with a copper mask, so that after an irradiation of one hour the film consists of an elastomer strip in the middle and two liquid strips of non-crosslinked material at both sides, see figure 2. The film is further irradiated after the liquid strips have been removed, for another hour.

We have not determined the optimum time necessary for crosslinking, so it is possible that much shorter irradiation times are sufficient for a complete crosslinking. We obtain a well oriented free-standing film attached to the support edges at two opposite sides [1, 8]. The smectic layers are parallel to the film surface. The films have the dimensions of about 2 mm (width) and 3–4 mm (length), and their in thickness is approximately 1 μm. The film thickness is not uniform, and the number of layers varies in the film plane. Polarized Fourier transform infrared (FTIR) spectroscopy is performed with an FTS-6000 FTIR (Bio-Rad) spectrometer in combination with an IR microscope (UMA-500 Bio-Rad). The size of the region chosen for the measurement is $250 \times 250\,\mu m^2$. The polarized IR beam propagates perpendicular to the film surface and to the smectic layers, see figure 3. The dependence of the IR spectra on the polarizer angle φ is measured in 9° steps from 0° to 180°. IR spectra are recorded with a spectral resolution of $4\,cm^{-1}$.

The films are uniaxially stretched in discrete steps and measurements are repeated after each step. The average in-plane strain is determined from the distance of the two fixed edges of the film. The temperature of the samples is controlled by a Linkam heating stage THMS 600. A typical IR spectrum is represented in figure 4. The assignment of the particular absorption lines to individual bond types in the molecule was achieved using standard methods [17].

3. Polarized FTIR measurements

The dependence of the absorbance A_v of a corresponding band v upon the orientation of the polarizer Ω gives detailed information on the average orientation of the bond and the orientational order of molecular segments

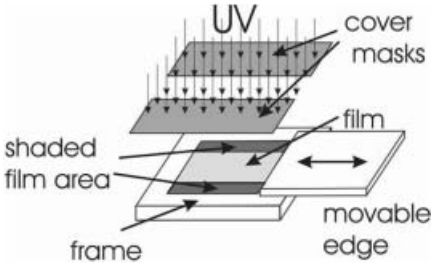

Figure 2. Schematic drawing of the film preparation set-up.

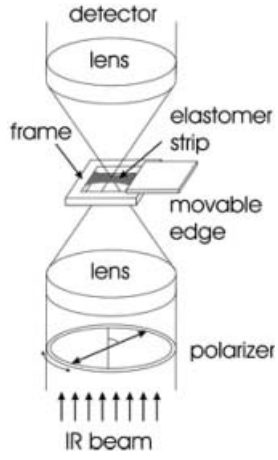

Figure 3. Schematic drawing of the set-up for polarized FTIR spectroscopy measurements of free-standing LCE films.

in the sample. The absorbance A_v is proportional to the scalar product $<(\varepsilon\mu)^2>$ where ε is the polarisation vector of the IR beam, μ is the molecular transition dipole moment [14–17], and the brackets indicate averaging over all molecules in the measured region. The dependence of the absorption on the polarizer angle is given by

$$A_v(\Omega) = A(\Omega_0)\cos^2(\Omega - \Omega_0) + A(\Omega_0 + 90^\circ)\sin^2(\Omega - \Omega_0) \quad (1)$$

where $A(\Omega_0)$ and $A(\Omega_0{+}90^\circ)$ define the main axes of the (time-averaged) projection of the absorbance ellipsoid in the layer plane, Ω_0 describes the mean bond orientation in the film plane and Ω is the orientation of the polarizer [22, 23].

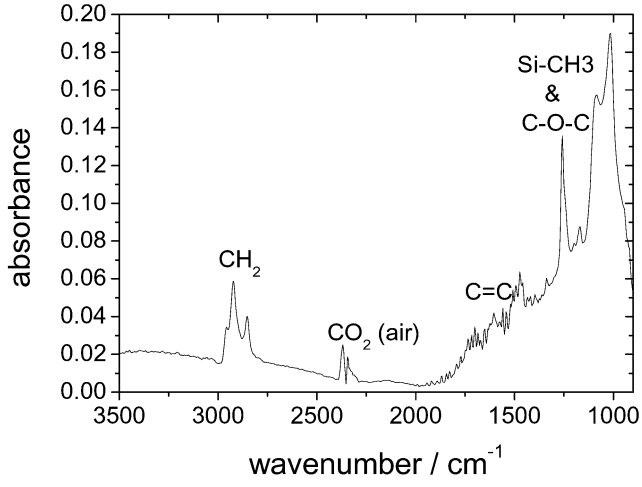

Figure 4. The infrared absorbance spectrum of a thin free-standing LCE film. The combinations of individual bond absorption peaks are indicated. The large background in the low wavenumber region is essentially contributed by water vapour in the path of the IR beam.

Introducing the parameters $a=[A(\Omega_0)+A(\Omega_0+90^\circ)]/2$ and $b=[A(\Omega_0)-A(\Omega_0+90^\circ)]/2$, the absorbance ellipsoid can be fitted by

$$A_v(\Omega)=a+b\cos 2(\Omega-\Omega_0). \quad (2)$$

The absorption bands of the CC and CH_2 groups are well separated, so the heights of the corresponding absorption peaks can be easily determined. The absorbances of the $SiCH_3$ and C–O–C bands overlap, so we will not consider them in the spectra evaluation. Figure 5 shows a polar plot of the measured absorbance dependence for the CC and CH_2 bands of the non-stretched film. We have to keep in mind that the absorbance depends on the number of molecules in the active area, i.e. on the film thickness. During stretching, the film thickness decreases while the area of the measuring spot as well as the density of the material remain the same, thus the amount of absorbing material in the IR beam decreases. We take this into account and correct the absorbances with a scaling factor proportional to the film thickness. However, this correction affects only the absolute absorption data but not their angular dependence, the latter being the most important feature for the following data evaluation.

From the isotropic rubber characteristics determined earlier [8], the correction factor is determined as follows: x_0, y_0, z_0 represent the initial dimensions of some arbitrary volume (stretching direction x, film normal z); $x'=x_0+\Delta x$, $y'=y_0+\Delta y$, $z'=z_0+\Delta z$ are the dimensions of the same volume element after mechanical deformation. From the volume conservation ($V=x_0y_0z_0=x'y'z'=const$) one has

$$\frac{x'y'z'}{x_0y_0z_0}=1. \quad (3)$$

In an isotropic material,

$$\frac{y'}{y_0}=\frac{z'}{z_0}=\left(\frac{x_0}{x'}\right)^{\frac{1}{2}}=\lambda_x^{-\frac{1}{2}} \quad (4)$$

where $\lambda_x=1+\varepsilon_x=x'/x_0$, $\varepsilon_x=\Delta x/x_0$ and Δx is the elongation along the stress axis. Film thicknesses L_{z0} and L_z, before and after stretching, respectively, are related by $L_z=L_{z0}\lambda_x^{-1/2}$. We multiply measured absorbances of stretched films by the factor $\lambda_x^{1/2}$, and refer to them in the following as corrected absorbances. Figure 6 represents corrected data for different deformations in SmA and SmC* phases. When the angular dependence of the absorbance is fitted with equation (2), we obtain the projections $A(\Omega_0)$ and $A(\Omega_0+90^\circ)$ of the main axes of the absorbance ellipsoid. We consider that the propagation of the IR beam is perpendicular to the smectic layers, and the polarization vector is in the smectic layer plane. In order to retrieve detailed information on the mesogen orientation, it is necessary to take into consideration the orientation of the bonds in the mesogens. Maximum and minimum absorptions, $A_\parallel$ when the electric field of the IR beam is along the maximum transition moment, and $A_\perp$ when the electric field is perpendicular to it, have been measured in earlier studies. It is established that the absorption ellipsoid of the CC bond has its maximum value parallel to the long axis of the mesogenic units and its minimum perpendicular to it, and quantitative data are available [17]. We can suppose that the minimum value of absorption measured in the smectic plane, $A(\Omega_0+90^\circ)$, corresponds in reasonable approximation to the minimum value of the CC absorption ellipsoid $A_\perp$.The value $A(\Omega_0)$ is, in accordance with equation (1), a combination of the absorptions parallel and perpendicular to the mesogen long axes, with coefficients depending on the

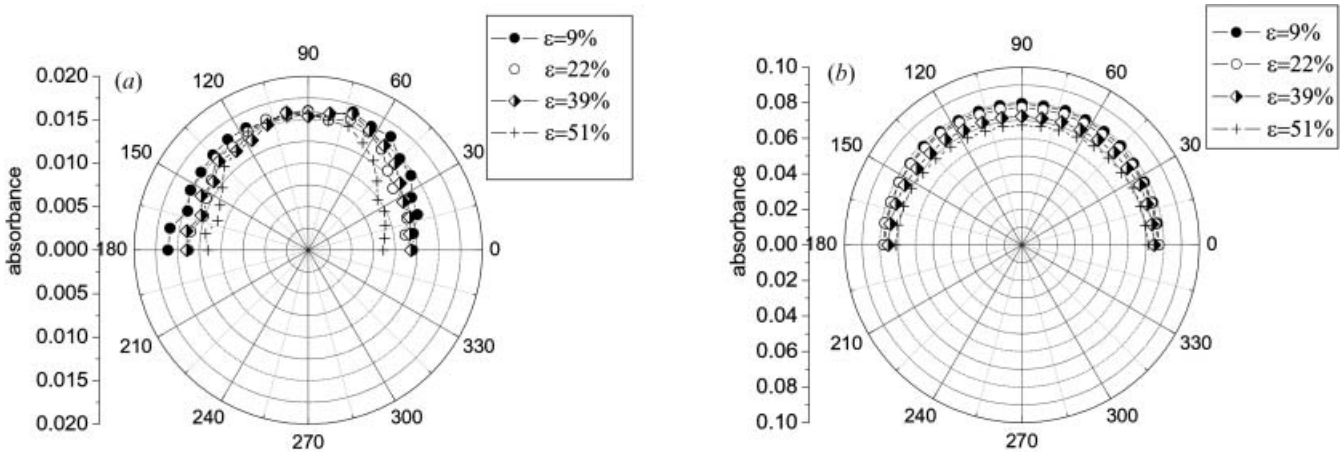

Figure 5. Polar plot of (*a*) CC and (*b*) CH_2 bond absorption for different values of deformation in the SmC* phase; uncorrected raw data.

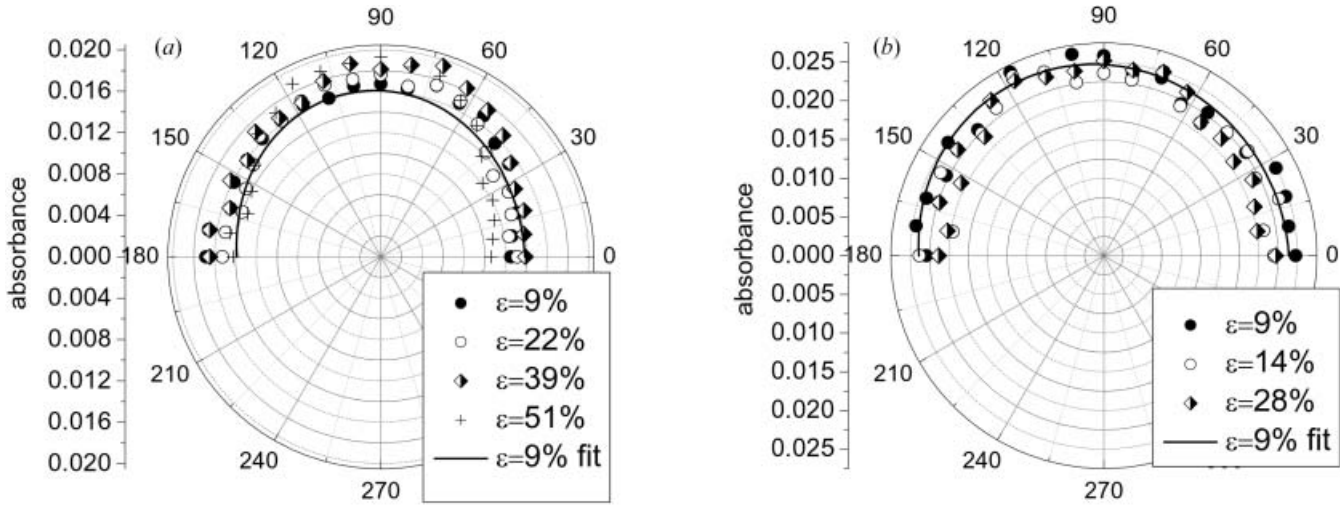

Figure 6. Polar plot of normalized absorbance for the CC bond in (*a*) SmC* and (*b*) SmA phases at different values of deformation, corrected with the film thickness changes in stretched films (see text). One fit curve (9% strain) is shown exemplarily.

angle between the electric field of the IR beam and the average orientation of the long axes of the mesogen units. For normal incidence, we obtain [17, 22, 23]

$$A(\Omega_0) = A_{\|} \sin^2(\phi_0) + A_{\perp} \cos^2(\phi_0) \qquad (5)$$

with the unknown angle ϕ_0 between the layer normal and the time-averaged bond direction, the geometry is sketched in figure 7.

Since both $A_{\|}$ and $A_{\perp}$ depend on the amount of material in the spot, which is not easily determined because of the inhomogeneity of the film thickness, we have no access to absolute absorbance values. Instead, we have to refer to their known ratio $R = A_{\|}/A_{\perp}$. From the measurements we can deduce only the value of the absorption ellipsoid perpendicular to the long axis of molecule, $A_{\perp}$. In stress-free films of the elastomer in an ordinary smectic A phase, the average orientation of the long axis of the mesogens is normal to the layers, $\phi_0 = 0$. There are some complications if the smectic A phase of the material is of the so-called de Vries type, as has been suggested earlier [24], the consequences will be discussed below. In order to estimate the value of the absorption ellipsoid parallel to the long axis of the mesogens, we employ the dichroic ratio $R_{CC} = A_{\|}/A_{\perp} = 5.4$ measured for CC bonds in similar materials [17]. From $A_{\perp} = A(\Omega_0 + 90^\circ)$ and known R_{CC} it is possible to determine $A_{\|}$ for a given film, to substitute $A(\Omega_0)$, $A_{\perp}$ and $A_{\|}$ into equation (5) and to determine the angle ϕ_0 between the average long axis of the mesogen units and the smectic layer normal. This procedure is useful only for the CC bond absorption line. Since the dichroic ratio for the CH_2 bonds is close to one, we do not consider the CH_2 absorption line for the further analysis.

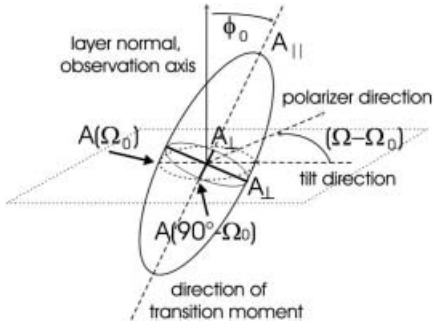

Figure 7. Absorbance ellipsoid and geometry in polarized FTIR spectroscopy measurements on free standing films. The film plane is indicated by the dashed parallelogram.

4. Results and discussion

FTIR measurements have been performed in the SmA and SmC* phases. Figure 6 shows polar plots of the polarized FTIR spectroscopy data of the CC bond for different film deformations in the SmC*, figure 6 (*a*), and SmA, figure 6 (*b*), phases. The films are stepwise stretched in the FTIR set-up, and the macroscopic strain at the individual steps is determined optically from photos of the film made before each FTIR measurement. The stretching direction is close to the angle $\Omega = 90^\circ$ on the polar diagrams of figure 6. The quantitative values of absorbance in the SmC* and SmA phases, figures 6 (*a*, *b*), cannot be compared directly because these measurements were made on two films with different thicknesses.

It is obvious from figure 6 that the absorbance of the CC bond is almost independent of the polarizer

orientation in both phases (modulations for different Ω less than 20%). In the SmC* phase, the absorbance in the film plane is only slightly anisotropic. If the SmC* film were a monodomain in the active spot, one would expect a much larger anisotropy (with the tilt angle of approximately 30° inserted in equation (5), the ratio of minimum and maximum should be close to 2). There are two possible explanations. Either the elastomer samples crosslinked in SmA develop a much smaller tilt angle when cooled into SmC*, or the multidomain structure of the sample averages out local anisotropies in the film plane to a great extend. The actual anisotropy of a few percent can be observed already at very small deformations of the film. The direction of maximum absorption is close to the stretching direction (for slight deviations, see below) and the anisotropy increases during stretching. However, the anisotropy does not change sufficiently to be considered responsible for the geometric changes of the sample. A quantitative analysis is presented below. In SmA, the almost circular graphs show that a stretching of the films up to almost 30% does not change the absorbance spectra qualitatively. There is neither a significant increment of the absorbance in the stretching direction, which would indicate that the mesogens tilt towards the stretching axis, nor is there an overall increase of the absorbance, which would indicate that the mesogens tilt in random directions to compensate the layer depression. In that case, the projection of the mesogen long axes on the layer plane would become larger, and the CC absorption bonds would increase correspondingly.

In order to estimate the change of the tilt angle in the SmA and SmC* phases quantitatively, we fit the experimental data of figure 6 with equation (2) with the average absorption a, the modulation b, and the angle Ω_0 of the absorbance maximum chosen as fit parameters.

From these parameters, we obtain the values $A(\Omega_0)$, $A(\Omega_0+90°)$ and Ω_0, which define the direction of the CC bond projected onto the smectic layer plane, and the mean mesogenic tilt θ. Figure 8 exemplarily shows the fit for the SmC* phase at a strain of $\varepsilon=39\%$.

The ratio $A(\Omega_0)/A(\Omega_0+90°)$, characterizing the anisotropy of the absorbance spectra and indicating changes of the mesogenic tilt, increases slightly with increasing deformation both in the SmC* and SmA phases. The angle for the maximum absorbance of the stretched sample in the SmC* phase is close to 100°, quite close but not exactly along the macroscopic stretching axis (direction normal to the clamp edges), and it does not change noticeably with increasing strain. In the SmA phase, this angle is difficult to measure at small deformations since the absorption is almost isotropic.

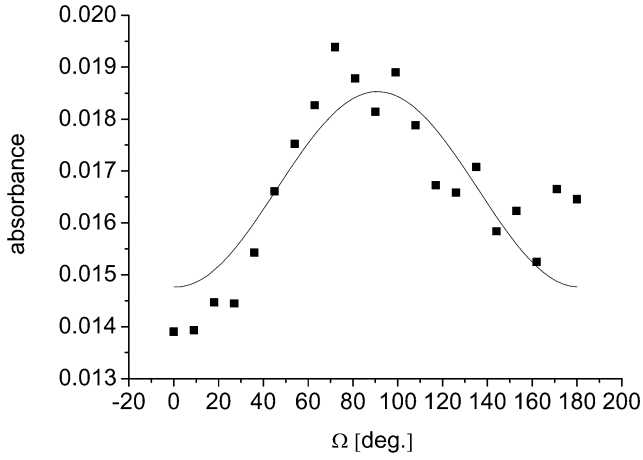

Figure 8. Fit of the IR absorbance spectrum in the SmC* phase at a strain $\varepsilon=39\%$ with the function from equation (2); parameters $a=0.01665$, $b=0.00188$, $\Omega=91°$.

As the film is increasingly stretched, the maximum locates near 100°, the experimental uncertainty becomes less than $\pm 3°$ for $\varepsilon=28\%$. The fact that the absorption maximum is close to 100° but not to 90°, i.e. in the global stretching direction, in both cases, may indicate that the local stretching axis of the film was not exactly normal to the clamp edges. This small deviation is not surprising, since the film deformation in the plane involves both expansion in the x- and contraction in the y-direction, it is strictly normal to the clamp edges only in the middle axis of the film.

In order to obtain the tilt angle of the mesogens as a function of film strain we have to consider the geometry of the absorbance ellipse in the tilt plane (figure 7). The absorbance in this plane can be described by equation (5), using experimentally obtained parameters $A(\Omega_0)$ and $A(\Omega_0+90°)$ and the dichroic ratio for the CC bond given above [17]. The angle ϕ_0 between layer normal and the long axis of the absorbance ellipsoid of the CC bond can thus be calculated. Under the assumption that the transition moment of the CC bond is along the mesogen long axis [17] ϕ_0 is equivalent to the tilt angle θ of the mesogens. Figure 9 shows tilt angles as a function of deformation obtained from the FTIR spectra for the SmC* (■) and SmA (□) phases.

The graphs of figure 9 give unambiguous evidence that the tilt angle creases with increasing deformation in the SmC* and SmA phases, but they indicate already that it is too small to be considered responsible for the observed geometric changes of the sample. This becomes even more obvious for the strain ε_x that could be achieved with the measured tilt angles, as opposed to the actual macroscopic strain of the samples, measured optically. With the relation $\cos^2\theta=\lambda_z^2=1/\lambda_x=1/(1+\varepsilon_{x\,tilt})$ valid for small strain, we calculate the

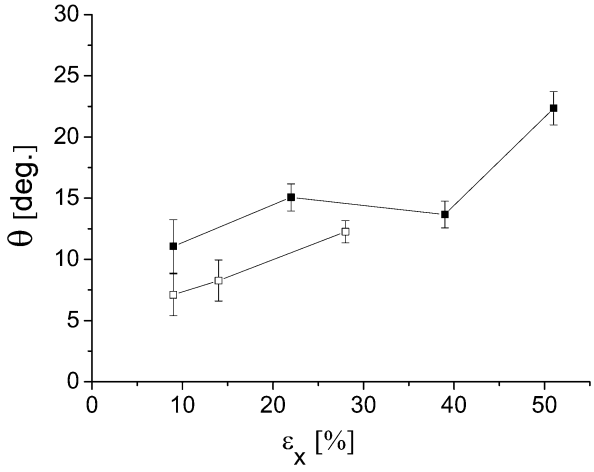

Figure 9. Tilt angle of the mesogens at different values of deformation in the SmC*(■) and SmA (□) phases, obtained from the polarized FTIR spectra; see equation (5).

(hypothetical) purely tilt induced strain $\varepsilon_{x,tilt}=\tan^2\theta$ that is shown in figure 10. The symbols (■) and (□) represent the strain that corresponds to an assumed compression of the layers with $\cos\theta$ in the SmC* and SmA phases, respectively, for comparison the straight line marks the actual strain.

Figure 11 represents a comparison of the smectic layer compression induced by lateral stretching, as obtained from X-ray measurements [8] with the hypothetical layer shrinkage related to the molecule tilt angle obtained from polarized FTIR spectroscopy. This figure gives unambiguous evidence that strain-induced tilt is too small to give a main contribution to the smectic layer compression.

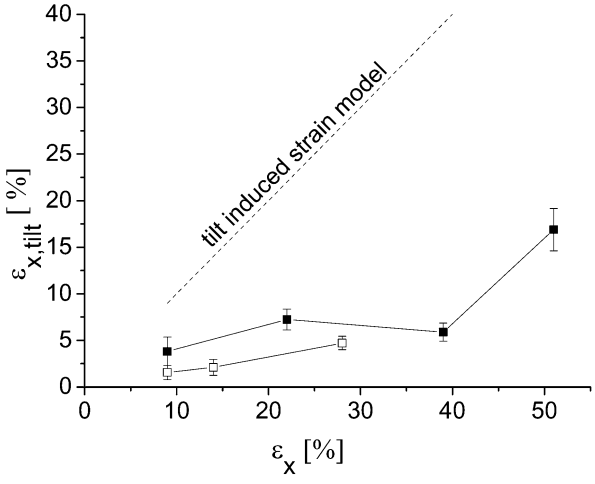

Figure 10. Comparison of the overall strain ε_x with the strain estimated from a pure tilt model for the SmC*(■) and SmA(□); $\varepsilon_{x,tilt}=\tan^2\theta$.

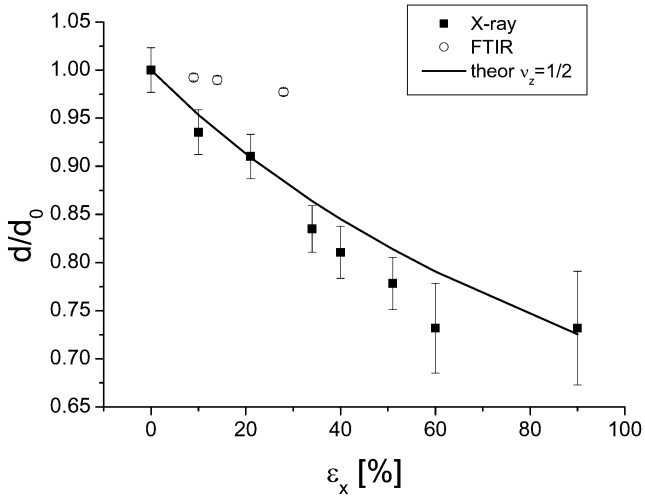

Figure 11. Comparison of the smectic layer compression d/d_0 obtained from X-ray (■) with data derived from the tilt angle measured by polarized FTIR spectroscopy (○) (d_0=smectic layer thickness of the non-stretched film, d=smectic layer thickness after deformation). The solid line represents the layer thickness vs. strain characteristics calculated for an isotropic material (Poisson ratio $v=1/2$).

It should be noted that this simplified model greatly overestimates the effects of an induced mesogen tilt on the layer shrinkage since, of the total layer structure, only the mesogenic part shrinks with increasing θ; the mesogenic tilt will not directly influence the siloxane and spacer layers. Thus, the actual effect of the measured tilt on the smectic layer thickness represents some upper estimate. The conclusion is that although there is a certain induced tilt towards the stretching axis, this tilt is by far insufficient to explain the layer shrinkage found from X-ray measurements and from the overall sample dimensions. Likewise, the rather unaffected absorption values indicate that the order parameter is not noticeably influenced by stretching the samples.

Several independent investigations have led to the conjecture that the material already has a tilt in the smectic A phase (de Vries type SmA) [13, 24, 25], with random azimuth. This assumption would be consistent with all the FTIR data presented above, except that the minimum absorbance in the SmA for normal incidence would not be equal to $A_\perp$ but to an intermediate value $A=A_\parallel\sin^2(\theta)+A_\perp\cos^2(\theta)$. Even if this assumption reflects the correct nature of the SmA structure in this class of elastomers materials, the conclusion remains valid that any additional strain-induced tilt can only to a small part be responsible for the observed layer shrinkage. Otherwise the absorbance of the CC line would increase much more with increasing strain, in

contrast to the data shown in figure 6 for the smectic A phase.

On a molecular level, we have to interpret this result in the following way: the main contribution to the sample deformation originates from a shrinkage of the layers at almost unchanged molecular orientations. This implies that the mesogens in adjacent layers interpenetrate the intermediate spacer and siloxane layers, so that the layer structure becomes softer. Even though a microscopic characterization of the network structure in the materials investigated is not available, we may speculate about the microscopic origin of the differences between the materials investigated in [6, 7] and those studied in [8–13]. In the first class of materials, the crosslinker distribution is not necessarily homogeneous on a nanometre scale, therefore an intact smectic structure and the large layer compression modulus dominate the elastic behaviour. In the second class of materials, the crosslinker density is probably much more uniform, as a consequence of the different cross linking strategy. In that case, the crosslinks act as homogeneously distributed distortions of the smectic structure in the stretched material, which may lead to a considerable suppression the of smectic (positional) order of the mesogenic units. This interpretation follows the ideas proposed in [26]. When the films are mechanically stretched, the crosslinks soften the layer structure, which then becomes easily distortable. A definite decision as to whether this model is correct would require a microscopic control of the crosslinker distribution, which is chemically very difficult and has not yet been achieved. After the solution of that problem, a deliberate manipulation of the mechanical types of LCE seems to be within reach.

Acknowledgements

This study was supported by the Deutsche Forschungsgemeinschaft within project STA 425/14 and by the European Regional Development Fund (ERDF).

References

[1] R. Köhler, R. Stannarius, C. Tolksdorf, R. Zentel. *Appl. Phys. A*, **80**, 381 (2005).
[2] W. Lehmann, H. Skupin, C. Tolksdorf, E. Gebhard, R. Zentel, P. Krüger, M. Lösche, F. Kremer. *Nature*, **410**, 447 (2001).
[3] W. Gleim, H. Finkelmann. In *Side Chain Liquid Crystalline Polymers*, C.B. McArdle (Ed.), Blackie and Son, Glasgow (1989); H. Finkelmann. In *Liquid Crystallinity in Polymers*, A. Ciferri (Ed.), VCH, Weinheim (1991).
[4] M. Warner, E.M. Terentjev. *Liquid Crystal Elastomers*, Oxford University Press (2003).
[5] H. Wermter, H. Finkelmann. *e-polymers*, no 13. http://www.e-polymer.org (2001).
[6] E. Nishikawa, H. Finkelmann. *Macromol. Chem. Phys.*, **200**, 312 (1999).
[7] E. Nishikawa, H. Finkelmann, H.R. Brand. *Macromol.rapid Commun.*, **18**, 65 (1997).
[8] V. Aksenov, J. Bläsing, R. Stannarius, M. Rössle, R. Zentel. *Liq. Cryst.*, **32**, 805 (2005).
[9] R. Stannarius, V. Aksenov, J. Bläsing, A. Krost, M. Rössle, R. Zentel. *Phys. Chem. chem. Phys.*, **8**, 2293 (2006).
[10] R. Stannarius, R. Köhler, M. Rössle, R. Zentel. *Liq. Cryst.*, **31**, 895 (2004).
[11] H. Schüring, R. Stannarius, C. Tolksdorf, R. Zentel. *Macromolecules*, **34**, 3962 (2001).
[12] R. Stannarius, R. Köhler, U. Dietrich, M. Lösche, C. Tolksdorf, R. Zentel. *Phys. Rev. E*, **65**, 041707 (2002).
[13] L. Naji, R. Stannarius, S. Grande, M. Rössle, R. Zentel. *Liq. Cryst.*, **32**, 1307 (2005).
[14] J. Prigann, Ch. Tolksdorf, H. Skupin, R. Zentel, F. Kremer. *Macromolecules*, **35**, 4150 (2002); M. Tammer, J. Li, A. Komp, H. Finkelmann and F. Kremer. *Macromol. Chem. Phys.*, **206**, 714 (2005).
[15] S.V. Shilov, H. Skupin, F. Kremer, T. Wittig, R. Zentel. *Phys. Rev. Lett.*, **79**, 1686 (1997).
[16] J. Li, M. Tammer, F. Kremer, A. Komp, H. Finkelmann. *Eur. Phys. J. E*, **17**, 423 (2005).
[17] H. Skupin. PhD thesis, University of Leipzig, Germany (2002).
[18] E.M. Terentjev. *J. Phys.: cond. Mat.*, **11**, R239 (1999).
[19] S. Shilov, E. Gebhard, H. Skupin, R. Zentel, F. Kremer. *Macromolecules*, **32**, 1570 (1999).
[20] H. Skupin, F. Kremer, S.V. Shilov, P. Stein, H. Finkelmann. *Macromolecules*, **32**, 3746 (1999).
[21] H. Wang, D.G. Thompson, J.R. Schoonover, S.R. Aubuchon, R.A. Palmer. *Macromolecules*, **34**, 7084 (2001).
[22] W.G. Jang, C.S. Park, J.E. Maclennan, K.H. Kim, N.A. Clark. *Ferroelectrics*, **180**, 213 (1996).
[23] B.K.P. Scaife, J.K. Vij. *J. chem. Phys.*, **122**, 174901 (2005).
[24] M. Rössle, R. Zentel, J.P.F. Lagerwall, F. Giesselmann. *Liq. Cryst.*, **31**, 883 (2004).
[25] C.C. Huang, S.T. Wang, X.F. Han, A. Cady, R. Pindak, W. Caliebe, K. Ema, K. Takekoshi, H. Yao. *Phys. Rev. E*, **69**, 041702 (2004).
[26] L. Radzihovski, J. Toner. *Phys. Rev. Lett.*, **78**, 4414 (1997); L. Radzihovski and J. Toner. *Phys. Rev. B*, **60**, 206 (1999).